

Chapter 3

The propagation of weak shock waves in non-ideal gas flow with radiation

“The only way to learn
mathematics is to do
mathematics.”

-Paul Halmos

3.1 Introduction

The analysis of asymptotic behaviour of the shock front location and the distribution of flow parameters in the shock wave zone is of great scientific and physical applications in the field of nuclear science, plasma physics, astrophysics, geophysics and interstellar gas masses etc. At very high temperature, the processes connected with emission dominant or absorption dominant of radiation influences the motion

of gas as it may cause change of composition of gas. The occurrence of discontinuities is a natural process in several areas such as photo ionized gas, space science, space re-entry vehicles, supernova explosions, collision of galaxies, stellar winds etc. Heat transfer is a special area of thermal engineering that concerns the conversion and exchange of thermal heat between physical system. As we know, heat transfer is classified into three mechanism such as thermal radiation, thermal convection and thermal conduction. Here, we study the heat transfer by thermal radiation in non-ideal gas flow. Heat transfer through radiation takes place in the form of electromagnetic waves mainly the infrared medium.

At the high temperature and too low density, the behaviour of idealness of the gas will not remain valid and the gas is governed by non-ideal gas model. The study of shock wave in non-ideal gas has gained importance in several industrial applications such as nuclear reactions, chemical processes, aerospace engineering and science etc. The investigation of shock related phenomena in non-ideal radiating gas is more complex phenomena than ideal gas. Therefore, in the presence of radiative heat transfer the flow takes place at high temperature and behaviour of idealness is no more valid. Hence, due to the effect of non-idealness parameter in the radiative gas flow produces significant result.

The investigation of asymptotic solution of the system of quasilinear hyperbolic PDE's plays important role to yield useful information for the understanding the complex physical phenomenon involved. By utilizing the theory of progressive wave analysis, the propagation of weakly non-linear waves have been discussed by several researchers in different gaseous media. The method of asymptotic analysis has been widely applied to study the propagation of weak shock waves modeled as the hyperbolic system of PDE's. Hunter and Keller [59] used the ray method to obtain weakly nonlinear high frequency wave solution of hyperbolic system. Fusco [37], Germain [38], Fusco and Engelbrecht [39], Sharma et al. [40], Singh et al. [41] and Nath

et al.[42, 43] have utilized the asymptotic technique to study the non-linear wave propagation in various gaseous media. Most of the physical phenomena occurring in the nature are determined with the help of mathematical models in terms of the hyperbolic system of PDE's [110, 19]. Choquet-Bruhat [111] have used the perturbation method to derive the shockless solution of hyperbolic system of PDE's based on single phase function.

A detailed discussion related to the propagation of discontinuous waves under the influence of radiation have been investigated by several researchers. In past, many attempts have been made to analyze the asymptotic properties of weak shock waves in various gasdynamic regimes where the governing equation is a system of quasilinear hyperbolic PDE's. The study of shock related phenomenon in non-ideal gas in the presence of radiative heat transfer or magnetic field was discussed by Nath et al. [112, 113, 114]. Singh et al. [70] have investigated the growth and decay behaviour of weak shock waves in an inviscid fluid with an added effect of magnetic field. Chaturvedi et al. [115] have analyzed the problem of weak shock waves in dusty gas using the method of wavefront analysis. Singh et al. [116] have applied the method of wavefront analysis to determine the propagation of weak shock waves in non-ideal gas with thermal radiation. By utilizing the perturbation theory, Pai and Hsieh [117] have discussed about an isentropic flow of a radiating gas approximated with optically thin limit. Singh et al. [118] used the perturbation technique to investigate the problem of propagation of weak shock waves in non-uniform medium with an added effect of radiation and magnetic field. Singh et al. [116] have studied the effect of thermal radiation on the propagation of weak shock waves in magnetogasdynamics. Singh et al. [119] have used an analytical approach to find an exact solution for the problem of weak shock waves in an ideal fluid with generalized geometry. Singh et al. [120] have investigated the problem of propagation of planar and non-planar weak shock waves in a non-ideal medium and obtained the analytical expression for

the shock formation distance. Seth et al. [121, 122, 122, 123, 124] have analyzed the effect of radiative heat transfer in Unsteady MHD free convection flow and heat and mass transfer flow with Hall effects. Also, Seth et al. [125, 126] and Bhattacharyya et al. [127] have studied the hydromagnetic natural convection casson fluid flow, entropy generation in hydromagnetic nanofluid flow and Cattaneo-Christov heat flux on the flow of single and multi-walled carbon nanotubes by using numerical and analytical approaches. The evolutionary behaviour of acceleration waves in different gaseous media is presented by Singh et al. [128, 129].

In all the above research works, the effect of radiation on the growth and decay process of the weak shock wave for the planar and non-planar non-ideal gas flow by using asymptotic approach have not been studied by any of the authors. The motive of the present study is to analyze the propagation of weak shock waves in the non-ideal radiating gas flow. The effect of radiation on the evolutionary process of the weak shock waves in non-ideal gas flow is also studied. Also, the influence of non-idealness on the decay process of weak shock wave is discussed. An asymptotic approach is utilized to investigate the propagation of weakly non-linear waves in non-ideal gas with radiation. Also the medium is considered to be sufficiently hot and radiative transfer equation is approximated under optically thin conditions. An evolution equation is derived here which describes the wave phenomenon in high frequency domain. Further, the behaviour of disturbances in the form of sawtooth wave obeying the non-ideal gas law under the influence of radiative transfer is analyzed. The effect of non-idealness parameter and radiation on the wave profiles is discussed here. Also, the length and velocity of sawtooth wave in both planar flow and cylindrically symmetric flow have been discussed here. In this theoretical work, we discuss the effect of radiation on the evolution of Half-N wave in non-ideal gas because the study of the effect of radiation plays an important role in energy transport over vast distances encountered between stellar objects, and can modify

the shock process.

This chapter is organized into sections as follows: In the second section, we determine the governing equations of motion and obtain the characteristics of the fundamental system of PDEs. In the third section, we discuss the asymptotic solution of the governing system of PDEs and obtain the shock formation time in the case of compressive waves. The analysis described in section three is used to analyze the behaviour of acceleration waves which is presented in the fourth section. In the fifth section, we obtain the R-H conditions for weak shock waves. The evolutionary behavior of a sawtooth wave is discussed in section six. The results and conclusion of this work are given in sections seven and eight respectively.

3.2 Problem Formulation and Characteristics

The equations governing the motion of one-dimensional unsteady planar flow and non-planar flow of a non-ideal radiating gas may be presented as follows [7, 9]

$$\frac{\partial \rho}{\partial t} + v \frac{\partial \rho}{\partial x} + \rho \frac{\partial v}{\partial x} + \frac{m \rho v}{x} = 0, \quad (3.1)$$

$$\frac{\partial v}{\partial t} + v \frac{\partial v}{\partial x} + \rho^{-1} \frac{\partial p}{\partial x} = 0, \quad (3.2)$$

$$\frac{\partial p}{\partial t} + v \frac{\partial p}{\partial x} + \rho c^2 \left[\frac{\partial v}{\partial x} + \frac{mv}{x} \right] + (\gamma - 1)R = 0. \quad (3.3)$$

where ρ and p stand for the fluid density and pressure respectively, x and t are the spatial coordinate and time respectively, v is the fluid velocity along the x -axis, c is the sound velocity which is defined as $c = \left(\frac{\gamma p}{\rho(1 - b\rho)} \right)^{1/2}$, with γ as the adiabatic index and b is the non-idealness parameter. Here R represents the rate of energy

loss by the gas per unit volume through radiation which is expressed as

$$R = 4k\Omega(T^4 - T_0^4), \quad (3.4)$$

where k is the Planck absorption co-efficient, Ω is the Stefan-Boltzmann constant and T_0 is constant state temperature. The effect of thermal radiation is approximated under the optically thin limit. The parameter m takes value 0 and 1 for planar and cylindrically symmetric flows respectively. Now the system of equations (3.1) to (3.3) are represented in the following matrix form as

$$\frac{\partial V}{\partial t} + P \frac{\partial V}{\partial x} + Q = 0, \quad (3.5)$$

where P is matrix of order 3×3 , V and Q are column vectors, written as

$$V = \begin{bmatrix} \rho \\ v \\ p \end{bmatrix}, P = \begin{bmatrix} v & \rho & 0 \\ 0 & v & \frac{1}{\rho} \\ 0 & \rho c^2 & v \end{bmatrix}, Q = \begin{bmatrix} \frac{m\rho v}{x} \\ 0 \\ (\gamma - 1)R + \frac{m\rho c^2 v}{x} \end{bmatrix}. \quad (3.6)$$

Now system (3.5) can be represented as

$$V_t^i + P^{ij} V_x^j + Q^i = 0, \quad i, j = 1, 2, 3. \quad (3.7)$$

The eigenvalues of the matrix P can be written as

$$\lambda_1 = v + c, \quad \lambda_2 = v - c, \quad \lambda_3 = v. \quad (3.8)$$

The left eigenvector and right eigenvector corresponding to the eigenvalue $v + c$ of the matrix P are

$$l^T = \begin{bmatrix} 0 \\ \rho c \\ 1 \end{bmatrix}, r = \begin{bmatrix} 1 \\ \frac{c}{\rho} \\ c^2 \end{bmatrix}, \quad (3.9)$$

where a superscript means transposition. Since the eigenvalues given by (3.8) are real and distinct and corresponding eigenvectors are linearly independent, therefore the above system of equations (3.7) will be strictly hyperbolic.

3.3 Progressive Wave Solutions

In this section, we discuss the asymptotic solution of Eq.(3.7) which represents the properties of progressive waves. The asymptotic expansion of the matrix V may be written in the following form

$$V^i(x, t) = V_0^i + \theta V_1^i(x, t, \omega) + O(\theta^2), \quad (3.10)$$

where V_0^i is constant solution of Eq.(3.7) which is known and satisfies the condition $B^i(V_0) = 0$. The other terms of Eq.(3.10) describe the nature of progressive wave. The preference of the parameter θ depends on the physical problem considered. Now we determine $\theta = \tau_{ch}/\tau_a \ll 1$, where τ_{ch} is the characteristic time scale of the medium and τ_a is the attenuation time scale. The variable ω is represented as $\omega = f(x, t)/\theta$, which is known as fast variable, where $f(x, t)$ is phase function which determines the wave front. It may be observed here that the condition $\theta \ll 1$ corresponds to the high frequency wave propagation where the attenuation frequency of the signal is very small as compared to the characteristic frequency of the medium [130].

Now, by introducing the Taylor's series expansion of P^{ij} and Q^i in the neighborhood

of known uniform solution V_0^i and utilizing Eq.(3.10), we obtain

$$P^{ij} = P_0^{ij} + \theta \left(\frac{\partial P^{ij}}{\partial V^k} \right)_0 V_1^k + O(\theta^2), \quad (3.11)$$

$$Q^i = \theta \left(\frac{\partial Q^i}{\partial V^k} \right)_0 V_1^k + O(\theta^2). \quad (3.12)$$

Now by using the Eqs.(3.10) to (3.12) in Eq. (3.7) and equating to zero the coefficient of θ^0 and θ^1 , we obtain the equations which are written as

$$(P_0^{ij} - \lambda \delta_j^i) \frac{\partial V_1^j}{\partial \omega} = 0, \quad (3.13)$$

$$(P_0^{ij} - \lambda \delta_j^i) \frac{\partial V_1^j}{\partial \omega} + \left(\frac{\partial V_1^i}{\partial t} + P_0^{ij} \frac{\partial V_1^j}{\partial x} \right) f_x^{-1} + V_1^k \left(\frac{\partial P^{ij}}{\partial V^k} \right)_0 \frac{\partial V_1^j}{\partial \omega} + f_x^{-1} V_1^k \left(\frac{\partial Q^i}{\partial V^k} \right)_0 = 0. \quad (3.14)$$

Here δ_j^i is the Krönecker delta, $\lambda = -f_t/f_x$, and the subscript 0 shows that the quantity involved is calculated at constant state V_0 . From Eq.(3.13), the characteristic polynomial is written as $\lambda^2(\lambda^2 - c_0^2) = 0$, where the eigenvalues $\pm c_0$ of P_0 are non-zero. The left and right eigenvectors of P_0 corresponding to eigenvalue $\lambda = c_0$, are written with the subscript 0 from Eq.(3.4). Now from Eq.(3.13) we observe that $\frac{\partial V_1}{\partial \omega}$ is collinear to r_0 , hence V_1 can be expressed as

$$V_1(x, t, \omega) = \beta(x, t, \omega)r_0 + S(x, t), \quad (3.15)$$

which describes the solution of Eq.(3.13). Here $\beta(x, t, \omega)$ is the amplitude factor which is to be calculated and the components of the vector S i.e. S^i are constants of integration and are not of the nature of progressive wave. So it may be equated to zero. Also the phase function i.e. $f(x, t)$ is written in the following form

$$f_t + c_0 f_x = 0, \quad (3.16)$$

and if $f(x, 0) = x - x_0$, then

$$f(x, t) = (x - x_0) - c_0 t. \quad (3.17)$$

Now, premultiplying Eq.(3.14) by l^i and after using Eq.(3.16) in resulting expression we have the following equation for β , which is used to analyze the evolution of the disturbance

$$\frac{\partial \beta}{\partial \tau} + A_0 \beta \frac{\partial \beta}{\partial \omega} + B_0 \beta = 0, \quad (3.18)$$

where $\frac{\partial}{\partial t} + c_0 \frac{\partial}{\partial x}$, is the ray derivative which is taken along the ray direction.

Here

$$A_0 = r_0^k \left(\frac{\partial(v+c)}{\partial V^k} \right)_0 = \frac{(\gamma+1)c_0}{2\rho_0(1-b\rho_0)} > 0, \quad (3.19)$$

$$B_0 = (l_0^i r_0^i)^{-1} \left((l_0^j r_0^k) \frac{\partial Q^i}{\partial V^k} \right)_0 = \frac{mc_0}{2x} + \frac{\Lambda}{c_0^2(\rho_0(1-b\rho_0))}, \quad (3.20)$$

where $\Lambda = 8k(\gamma-1)\alpha$, represents the effect of thermal radiation with $\alpha = \sigma_0(\gamma-1)T_0^4$, as the Boltzmann number representing the rate of convective energy flux to the black body heat flux. Here, the quantity $\left(\frac{\Lambda}{c_0^2 \rho_0 (1-b\rho_0)} \right)^{-1}$, has the dimension of time and it can be taken as having the attenuation time τ_a characterizing the medium. Eq.(3.18) is hyperbolic in nature and its characteristics curve can be written as

$$\omega = \omega_0 + \tau A_0 \left(\frac{-\Lambda}{c_0^2 \rho_0 (1-b\rho_0)} \exp \left[\frac{-\Lambda \theta}{c_0^2 \rho_0 (1-b\rho_0)} \right] \right) \phi(x_0, \omega_0), \quad (m=0) \quad (3.21)$$

$$\omega = \omega_0 + \frac{A_0 \phi(x_0, \omega_0) \frac{x_0}{c_0} \exp \left[\frac{\Lambda x_0}{c_0^3 \rho_0 (1-b\rho_0)} \right] \left(-1 + \operatorname{erf} \left[\frac{\Lambda}{c_0^3 \rho_0 (1-b\rho_0)} \right] \right)}{\left(\frac{x_0}{\Pi(x_0 + c_0 \tau)} \right)^{1/2} \left(\frac{\Lambda(x_0 + c_0 \tau)}{c_0^3 \rho_0 (1-b\rho_0)} \right)}. \quad (m=1) \quad (3.22)$$

Further, the existence of an envelope of the characteristics given by Eq. (3.21) and Eq. (3.22) provide the information about the shock formation. Therefore, the characteristics satisfying the condition $\frac{\partial\phi}{\partial\omega_0} < 0$, i.e. $\tau > 0$, will generate the shock wave. The time when first shock is formed in case of compressive waves can be written as

$$\tau_{sh} = \min \left(\frac{-\Lambda}{c_0^2 \rho_0 (1 - b\rho_0)} \exp \left[\frac{-\Lambda\tau}{c_0^2 \rho_0 (1 - b\rho_0)} \right] \left| \frac{\partial\phi}{\partial\omega_0} \right| \right)^{-1},$$

(for plane flow)

(3.23)

$$\tau_{sh} = \min \left(\frac{x_0}{c_0} \left[\frac{1}{x_0} \left[A_0 \frac{x_0^{1/2} \pi^{1/2}}{\Lambda} c_0^2 \rho_0 (1 - b\rho_0) \exp \left[\frac{\Lambda x_0}{B1} \right] \left| \frac{\partial\phi}{\partial\omega_0} \right| \left(-1 + \operatorname{erf} \left[\frac{\Lambda}{B1} \right] \right) \right]^{-1/2} - 1 \right] \right),$$

(for cylindrically symmetric flow)

(3.24)

where $B1 = c_0^3 \rho_0 (1 - b\rho_0)$.

3.4 Acceleration Waves

In this section, the analysis presented in section 3 is used to analyze the behaviour of acceleration waves. We represent the acceleration front by the curve $f(x, t) = 0$. Velocity is continuous across acceleration front but its derivatives admit jump discontinuities. Now, in the neighbourhood of the acceleration front the velocity v can be written as

$$v = \theta v_1(x, t, \omega) + O(\theta^2). \quad (3.25)$$

Here, $v_1 = 0$ and $v_1 = O(\omega)$, for $\omega < 0$ and $\omega > 0$ respectively. From Eq.(3.15), v_1 is an element of column vector V_1 . So, we obtain

$$\beta(x, t, \omega) = \begin{cases} 0, & \text{if } \omega < 0, \\ \omega\alpha(x, t) + O(\omega^2), & \text{if } \omega > 0, \end{cases} \quad (3.26)$$

where $\alpha = \left(\frac{\rho_0}{c_0}\sigma\right)$ with $\sigma = \left[\frac{\partial v}{\partial x}\right]$, represents the jump in velocity gradient across the acceleration front.

In view of Eq.(3.26), Eq.(3.18) results in the following Bernoulli-type ordinary differential equation at the front $f(x, t) = 0$, i.e. $\omega = 0$,

$$\frac{d\sigma}{dt} + B_0\sigma + \Pi_0\sigma^2 = 0. \quad (3.27)$$

$$\text{Here, } \Pi_0 = \frac{(\gamma + 1)}{2(1 - b\rho_0)} \text{ and } B_0 = \frac{mc_0}{2x} + \frac{\Lambda}{c_0^2\rho_0(1 - b\rho_0)}.$$

The solution of differential equation Eq.(3.27) for $m = 0$ and $m = 1$ respectively, is obtained as

$$\sigma = \frac{\sigma_0 \exp\left[\frac{-\Lambda t}{c_0^2\rho_0(1 - b\rho_0)}\right]}{1 + \sigma_0\Pi_0 \frac{c_0^2\rho_0(1 - b\rho_0)}{\Lambda} \left(1 - \exp\left[\frac{-\Lambda t}{c_0^2\rho_0(1 - b\rho_0)}\right]\right)}, \quad (m = 0), \quad (3.28)$$

$$\sigma = \frac{\sigma_0 \left(1 + \frac{c_0 t}{x_0}\right)^{-1/2} \exp\left[\frac{-\Lambda t}{c_0^2\rho_0(1 - b\rho_0)}\right]}{1 + \sigma_0\Pi_0 x_0^{1/2} \left(\frac{\pi c_0\rho_0(1 - b\rho_0)}{\Lambda}\right)^{1/2} \exp\left[\frac{\Lambda x_0}{B1}\right] \operatorname{erfc}\left[\frac{\Lambda x_0}{B1}\right]^{1/2} * K}, \quad (m = 1), \quad (3.29)$$

where, $B1 = c_0^3 \rho_0 (1 - b\rho_0)$ and $K = \left(1 - \frac{\operatorname{erfc} \left[\frac{\Lambda(x_0 + c_0 t)}{B1} \right]^{1/2}}{\operatorname{erfc} \left[\frac{\Lambda x_0}{B1} \right]^{1/2}} \right)$.

3.5 Weak Shock

The aforementioned analysis represents that after a finite time a compressive pulse always culminates into shock wave, however it may be weak initially. The flow variables ahead of the shock wave are represented by the subscript 0 and behind of the shock wave are represented by the subscript 1. Now by introducing the shock strength parameter $\delta = \frac{(\rho_1 - \rho_0)}{\rho_0}$, flow and field variables satisfy the following Rankine-Hugoniot conditions

$$\rho_1 = \rho_0(1 + \delta), v_1 = \frac{\delta G}{(1 + \delta)}, p_1 = p_0 + \frac{\delta}{(1 + \delta)} \rho_0 G^2, \quad (3.30)$$

where the shock velocity G and shock strength parameter δ are related by

$$G^2 = \frac{2c_0^2(1 + \delta)}{2(1 - b\rho_0\delta) - \delta(\gamma - 1)(1 + b\rho_0)}. \quad (3.31)$$

For a weak shock wave $\delta \ll 1$, the first approximation of Eq. (3.30) and Eq. (3.31) yield

$$\rho_1 = \rho_0(1 + \delta), v_1 = c_0\delta, p_1 = p_0(1 + \gamma\delta), \quad (3.32)$$

$$G = c_0 \left(1 + \frac{\Pi_0\delta}{2} \right). \quad (3.33)$$

3.6 Behaviour of weak shock wave in the form of sawtooth wave

The sawtooth wave (half N-wave) is generated after traveling the long distance from the body moving with supersonic speed [19]. As a result the shock wave propagated initially becomes sufficiently weak and one may utilize the weak shock wave relations Eq.(3.32) [33]. Therefore we consider that the shock wave is sufficiently weak at the beginning and analyze the advancement of disturbance which is represented in the shape of half N-wave depicted in Fig.3.1. In the beginning, the left segment of the half N-wave placed at point x_0 and travels with speed c_0 in the medium at rest however the right segment of half N-wave placed initially at point x_s which moves faster. Let us consider that L_0 is the initial length of the half N-wave. By hiding the subscript 1, we denote v and c by the state at the rear side of the shock, whose position at time t is given as:

$$x_s(t) = x_0 + c_0 t + L(t),$$

where $L(t)$ represents the length of the half N-wave at any time t . Then

$$G = \frac{dx_s}{dt} = c_0 + \frac{dL}{dt}. \quad (3.34)$$

Now, with the help of Eq. (3.32) and Eq. (3.33), we have

$$G = c_0 + \frac{v\Pi_0}{2}. \quad (3.35)$$

In the half N-wave, the fluid velocity v with constant $\frac{\partial v}{\partial x}$ can be written as

$$v = \sigma L(t). \quad (3.36)$$

Here, $\sigma = \left(\frac{\partial v}{\partial x} \right)_{x-x_0=c_0t}$, is the slope of half N-wave at any time t which is given by Eq.(3.28) and Eq. (3.29). Now by introducing Eq.(3.36) in Eq.(3.35) and comparing the resulting expression with Eq.(3.34), we get the following equation

$$\frac{dL}{dt} = \frac{\sigma L \Pi_0}{2}. \quad (3.37)$$

Let us consider that σ_0 , L_0 and G_0 represent the value of σ , L and G at time $t = 0$ respectively. Further, when we solve the Eq.(3.35) and Eq.(3.36) at time $t = 0$, we obtain the following relation

$$\sigma_0 = \frac{2(G_0 - c_0)}{L_0 \Pi_0}. \quad (3.38)$$

Now, with the help of Eq.(3.28) and Eq.(3.37) we obtain the length of sawtooth wave in the following form

$$L = L_0 \left[1 + \frac{\Pi_0 \sigma_0 c_0^2 \rho_0 (1 - \bar{b})}{\Lambda} \left(1 - \exp \left[\frac{-\Lambda t}{c_0^2 \rho_0 (1 - \bar{b})} \right] \right) \right]^{1/2}, \quad (m = 0), \quad (3.39)$$

$$L = L_0 \left[1 + \Pi_0 \sigma_0 t x_0^{-1/2} \left(1 + \sigma_0 \Pi_0 \left(\frac{\pi c_0 \rho_0 (1 - \bar{b})}{\Lambda} \right)^{1/2} \exp \left[\frac{\Lambda x_0}{B1} \right] \operatorname{erfc} \left[\frac{\Lambda x_0}{B1} \right]^{1/2} * K \right) \right]^{1/2}, \quad (m = 1), \quad (3.40)$$

$$\text{where } K = \left(1 - \frac{\operatorname{erfc} \left[\frac{\Lambda(x_0 + c_0 t)}{B1} \right]^{1/2}}{\operatorname{erfc} \left[\frac{\Lambda x_0}{B1} \right]^{1/2}} \right) \text{ and } \bar{b} = b \rho_0.$$

Further, by utilizing the Eqs.(3.28), (3.39) and (3.40) in Eq.(3.36), the velocity of half N-wave is given by

$$\frac{v}{v_0} = \frac{\exp \left[\frac{-\Lambda t}{c_0^2 \rho_0 (1 - \bar{b})} \right]}{\left[1 + \frac{\Pi_0 \sigma_0 c_0^2 \rho_0 (1 - \bar{b})}{\Lambda} \left(1 - \exp \left[\frac{-\Lambda t}{c_0^2 \rho_0 (1 - \bar{b})} \right] \right) \right]^{1/2}},$$

(m = 0), (3.41)

$$\frac{v}{v_0} = \frac{\exp \left[\frac{-\Lambda t}{c_0^2 \rho_0 (1 - \bar{b})} \right] \left(1 + \frac{c_0 t}{x_0} \right)^{-1/2}}{\left[1 + \Pi_0 \sigma_0 t x_0^{-1/2} \left(1 + \sigma_0 \Pi_0 \left(\frac{\pi c_0 \rho_0 (1 - \bar{b})}{\Lambda} \right)^{1/2} \exp \left[\frac{\Lambda x_0}{B1} \right] \operatorname{erfc} \left[\frac{\Lambda x_0}{B1} \right]^{1/2} K \right) \right]^{1/2}},$$

(m = 1). (3.42)

3.7 Results and discussion

The length and velocity curves of the sawtooth wave (Half N- wave) for planar and cylindrically symmetric flows are given by Eq.(3.39) to Eq.(3.42). Corresponding computed values are presented in Figs. 3.2 to 3.7 for different values of parameters of non-idealness and radiative heat transfer. Here, we have used MATHEMATICA 11.1 to compute the values. The effect of radiation and non-idealness enters into the solution through the parameters Λ and \bar{b} respectively. It is noticed here that the length of half N-wave increases faster with respect to time in planar flow as compared to cylindrically symmetric flow.

Fig. 3.2 and Fig. 3.3 represent the variation of length of half N-wave for planar and cylindrically symmetric flows respectively under the effect of non-idealness parameter and radiation. We observe that the presence of non-idealness parameter causes to enhance the length of half N-wave. The effect of increasing values of non-idealness

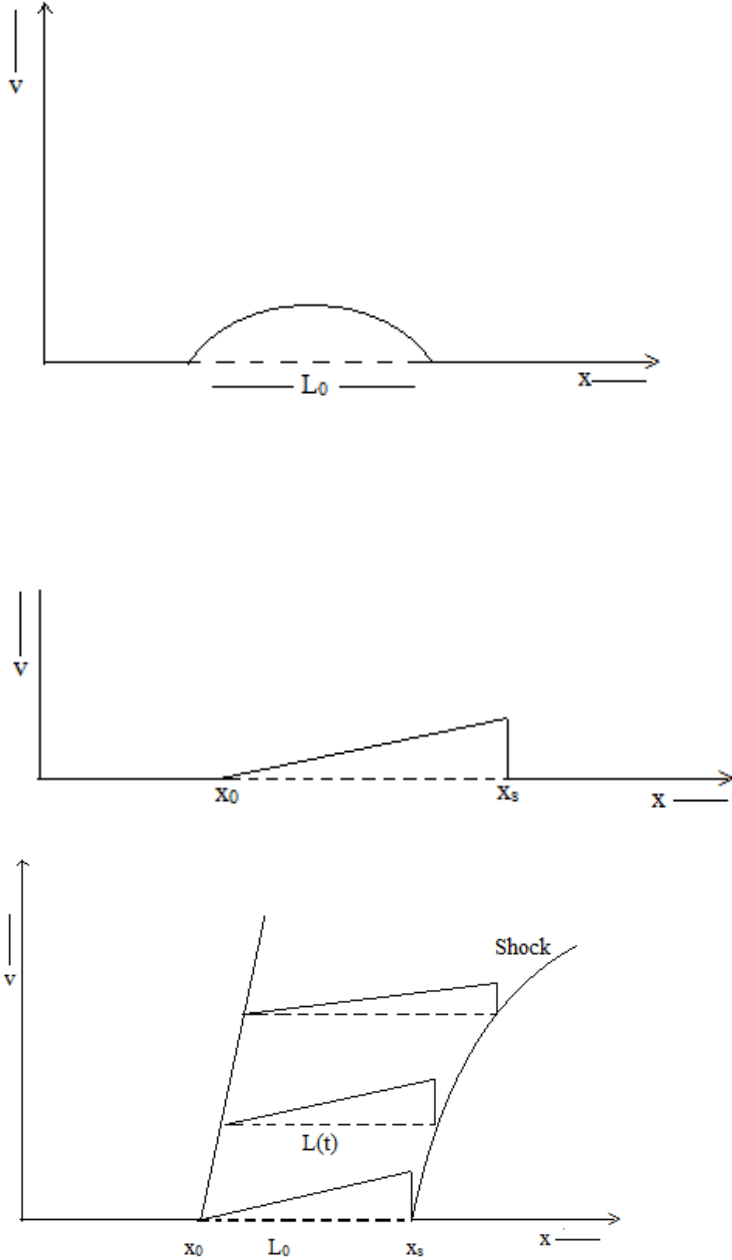


FIGURE 3.1: Formation and decay of Sawtooth wave (Half N-wave)

parameter is to further increase the length of half N-wave i.e. it will enhance the process of decay of shock wave. The curves 3 and 4 represent that the effect of non-idealness parameter causes to increase the length of half N-wave faster as compared to in case of radiative transfer. Further, the effect of non-idealness is to destabilize the shock wave whereas the effect of radiation is to stabilize the shock wave in due course of time.

Fig. 3.4 and Fig. 3.5 represent the velocity of sawtooth wave for planar and cylindrically symmetric flow respectively under the effect of non-idealness parameter and radiation. The velocity of half N-wave decreases faster with time in cylindrically symmetric flow as compared to planar flow. It is noticed here that the effect of increasing values of non-idealness parameter is to decrease the velocity of half N-wave, i.e. it will enhance the process of decay of shock wave. We observe that the addition of radiation effect accelerates the decay of half N-wave. The combined effect of radiation and non-idealness causes the decaying process of the shock wave to further hastened.

Fig. 3.6 and Fig. 3.7 represent the effect of radiation on the length and velocity of sawtooth wave in the presence of non-idealness parameter $\bar{b} = 0.4$ for planar and cylindrically symmetric flows respectively. We note that the effect of increasing values of radiation parameter is to decrease the length of half N-wave whereas the same effect gives a decreasing trend in the velocity of sawtooth wave. Hence, the radiation has the stabilizing effect on the shock. Further, the study of the effect of interaction of non-idealness of the gas and radiative heat transfer is of special interest to the physicist working in the area of space science, astrophysics and high temperature gas dynamic phenomenon. Further, in the absence of radiative heat transfer results obtained here agree closely with the earlier results [41]. Also, it is found that the result obtained in this study for $\bar{b} = 0$ is in close agreement with the result presented in the literature [131] in the absence of magnetic field.

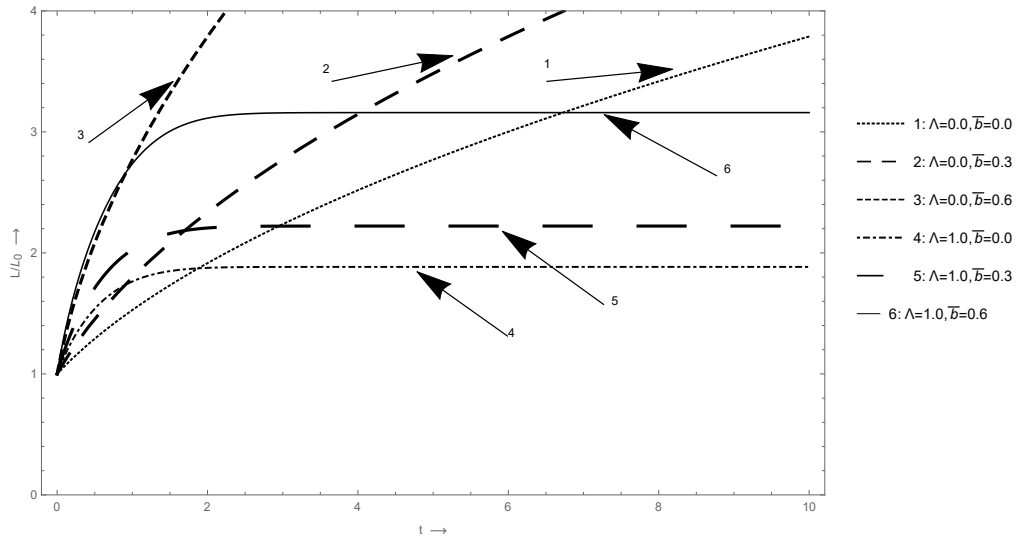


FIGURE 3.2: Length L/L_0 of sawtooth wave (Half N-wave) with respect to time t for planar flow.

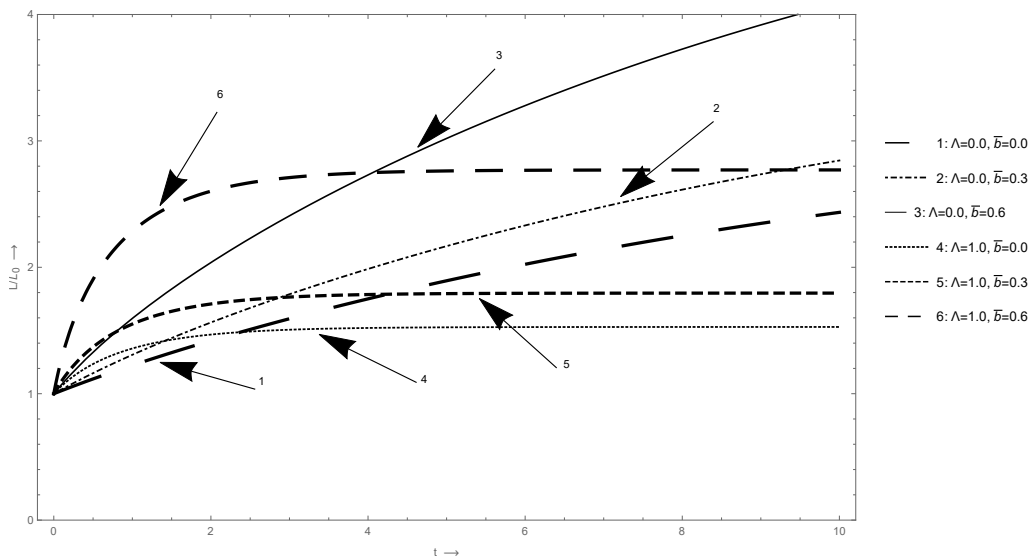


FIGURE 3.3: Length L/L_0 of sawtooth wave (Half N-wave) with respect to time t for cylindrically symmetric flow.

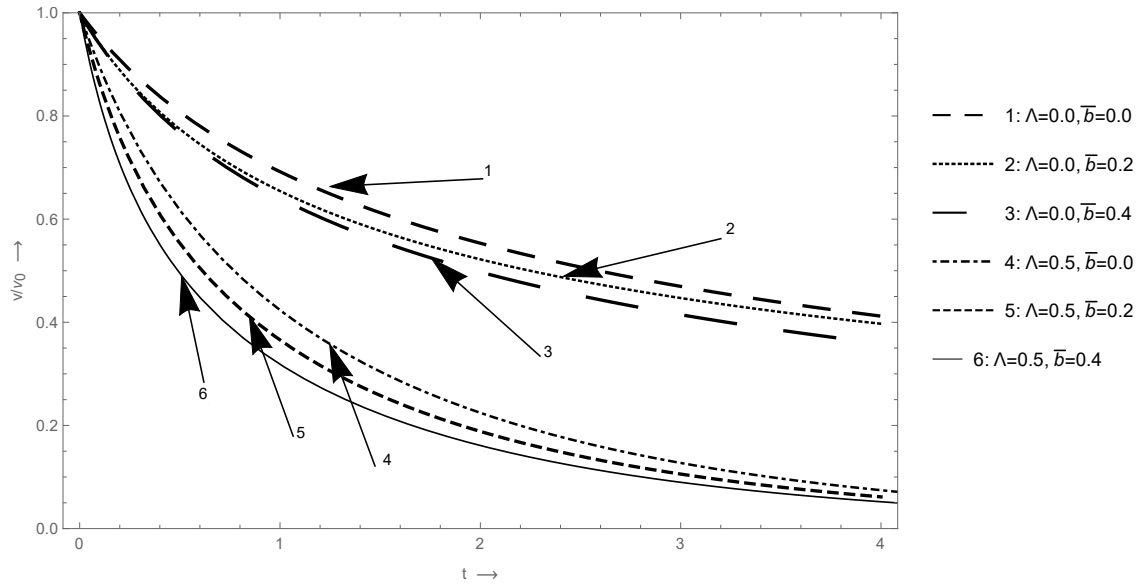


FIGURE 3.4: Variation of velocity v/v_0 of sawtooth wave (Half N-wave) with respect to time t for planar flow.

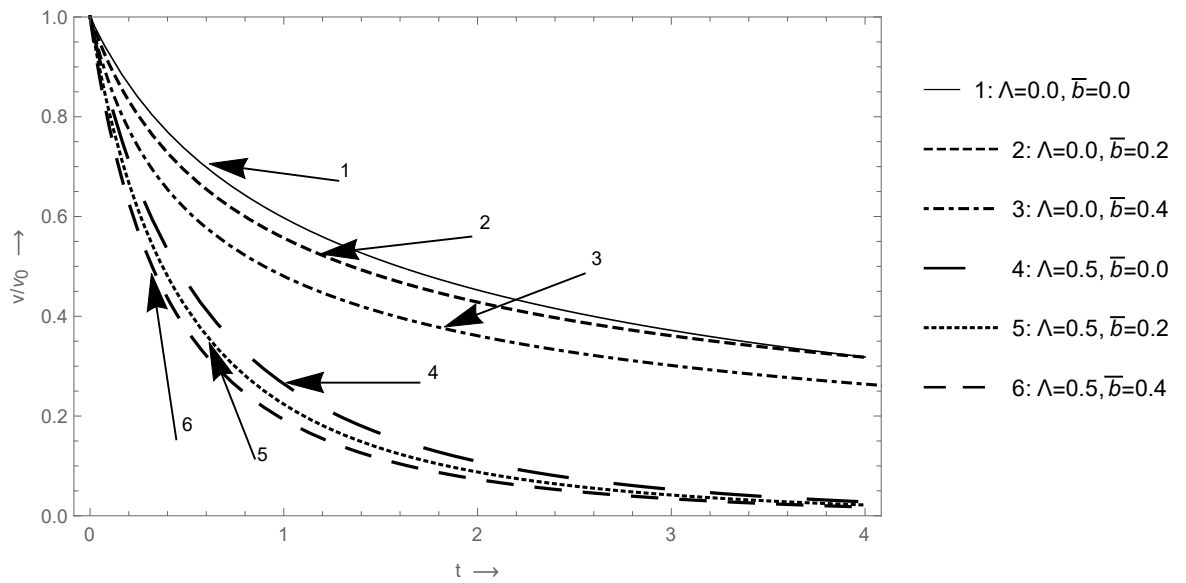


FIGURE 3.5: Variation of velocity v/v_0 of sawtooth wave (Half N-wave) with respect to time t for cylindrically symmetric flow.

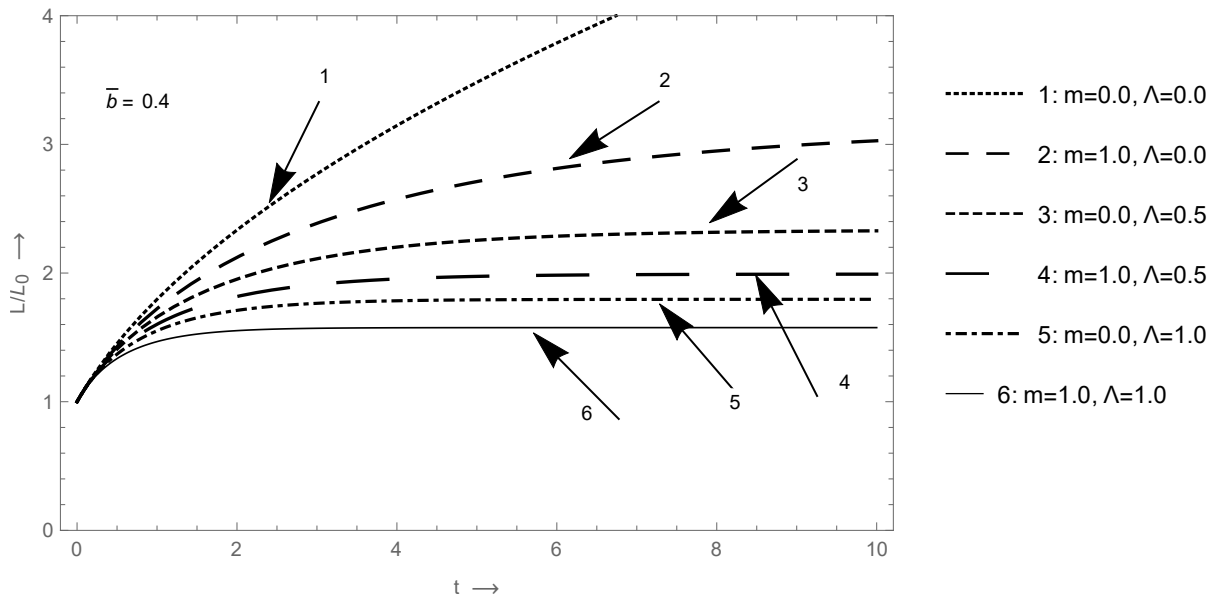


FIGURE 3.6: Length L/L_0 of sawtooth wave (Half N-wave) with respect to time t in the presence of non-idealness parameter $\bar{b} = 0.4$.

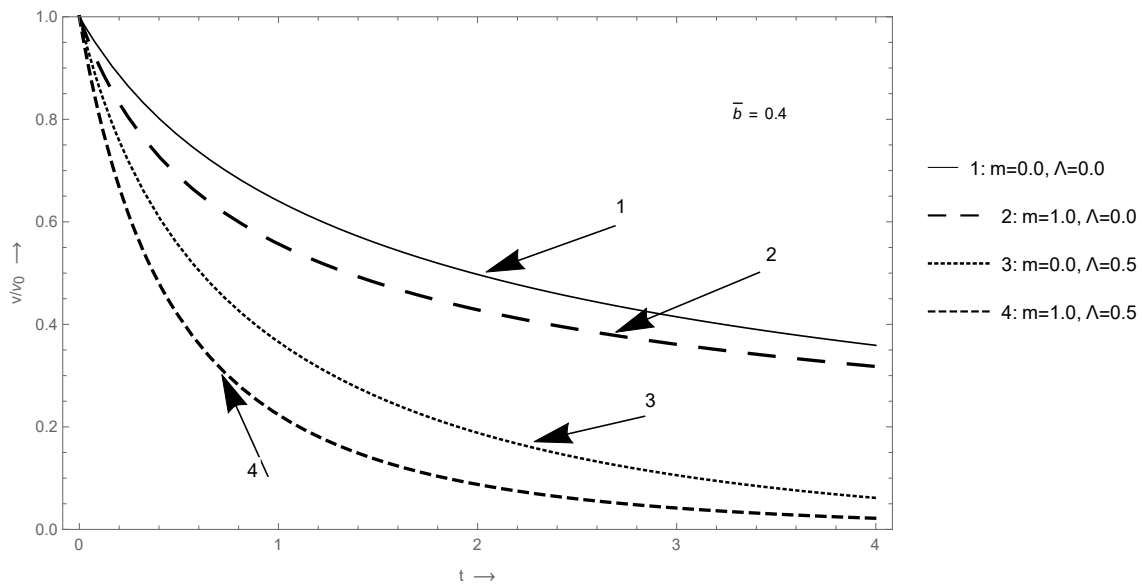


FIGURE 3.7: Velocity v/v_0 of sawtooth wave (Half N-wave) with respect to time t in the presence of non-idealness parameter $\bar{b} = 0.4$.

3.8 Conclusion

The method of progressive wave analysis is used to study the main features of weakly non-linear waves propagating in a compressible, inviscid non-ideal radiating gas flow. Here, a sufficiently weak shock is taken at the front and we analyze the motion of the weak shock wave in the form of sawtooth wave (half-N wave). Further, an evolution equation is derived which describes the propagation of disturbance in high frequency domain and determine the condition for the formation of shock wave at a finite time. For the effect of radiation, the radiative transfer equation is approximated under the optically thin limit. We analyze the length and velocity of sawtooth (half N-wave) for planar and cylindrically symmetric flows in non-ideal radiating gas. We observed that the effect of increasing values of non-idealness parameter is to further increase the length of half N-wave i.e. it will enhance the process of decay of shock wave. We analyzed that the effect of increasing values of radiation parameter is to decrease the length of half N-wave whereas the same effect gives a decreasing trend in the velocity of sawtooth wave. Further, the length of half N-wave increases faster with respect to time in planar flow as compared to cylindrically symmetric flow. The effect of increasing values of non-idealness parameter is to decrease the velocity of half N-wave, i.e. it will enhance the process of decay of shock wave. The velocity of half N-wave decreases faster with time in cylindrically symmetric flow as compared to planar flow. The addition of radiation effect accelerates the decay of half N-wave. We observe here that the combined effect of non-idealness and radiation causes to further enhance the decay process of sawtooth wave. Hence, the non-idealness parameter is to destabilize the shock wave whereas the effect of radiation is to first destabilize the shock and then stabilize the shock in due course of time. Further, the results obtained here were validated with the earlier works existing in the literature.
